

Perception-Oriented Single Image Super-Resolution using Optimal Objective Estimation - Supplementary Material

Seung Ho Park^{1,2}, Young Su Moon², Nam Ik Cho^{1,3}

¹Department of Electrical and Computer Engineering, INMC, Seoul National University, Korea

²Visual Display Division, Samsung Electronics, Korea

³IPAI, Seoul National University, Korea

1. More Visual Comparisons of SISR 4×

We provide more visual comparisons of 4× SISR between our proposed SROOE and other state-of-the-art methods including a distortion-oriented method, RRDB [7], and perception-oriented methods, such as SRGAN [2], ESRGAN [7], SFTGAN [6], RankSRGAN [8], SRFlow [3], SPSR [4], in Fig. from 1 to 6. Among the seven perception-oriented SR methods, the best performances are highlighted in red.

2. Performance Comparison of SISR 8×

Quantitative Comparison. Table 1 shows the quantitative performance comparison for 8× SISR. We compared it with a distortion-oriented method, RRDB [7], and perception-oriented methods, such as ESRGAN [7], SRFlow [3], and FxSR [5]. The table shows that our method yields the best results among the perception-oriented methods on all datasets, in terms of PSNR, SSIM, LPIPS and DISTS [1]. However, in LR-PSNR, unlike SR 4×, less than 45 dB indicates that LR consistency needs improvement.

Qualitative Comparison. Fig. 7 and Fig. 8 show visual comparisons, where we can observe that SROOE generates more accurate and cleaner structures with less unnatural details. Among the four perception-oriented SR methods, the best performances are highlighted in red.

3. Performance comparison of SR results of ESRGAN models with different weight vectors for perceptual loss

Table 2 shows the data before normalization. Min-max normalization used for Table 1 in the main paper used is as follows:

$$x' = (x - \min(x)) / (\max(x) - \min(x)). \quad (1)$$

References

- [1] Keyan Ding, Kede Ma, Shiqi Wang, and Eero P. Simoncelli. Image quality assessment: Unifying structure and texture similarity. *IEEE Transactions on Pattern Analysis and Machine Intelligence*, pages 1–1, 2020. 1
- [2] Christian Ledig, Lucas Theis, Ferenc Huszár, Jose Caballero, Andrew Cunningham, Alejandro Acosta, Andrew Aitken, Alykhan Tejani, Johannes Totz, Zehan Wang, et al. Photo-realistic single image super-resolution using a generative adversarial network. In *Proceedings of the IEEE conference on computer vision and pattern recognition*, pages 4681–4690, 2017. 1
- [3] Andreas Lugmayr, Martin Danelljan, Luc Van Gool, and Radu Timofte. SrfLOW: Learning the super-resolution space with normalizing flow. In *European Conference on Computer Vision*, pages 715–732. Springer, 2020. 1, 8
- [4] Cheng Ma, Yongming Rao, Yean Cheng, Ce Chen, Jiwen Lu, and Jie Zhou. Structure-preserving super resolution with gradient guidance. In *Proceedings of the IEEE/CVF Conference on Computer Vision and Pattern Recognition*, pages 7769–7778, 2020. 1
- [5] Seung Ho Park, Young Su Moon, and Nam Ik Cho. Flexible style image super-resolution using conditional objective. *IEEE Access*, 10:9774–9792, 2022. 1, 8
- [6] Xintao Wang, Ke Yu, Chao Dong, and Chen Change Loy. Recovering realistic texture in image super-resolution by deep spatial feature transform. In *Proceedings of the IEEE conference on computer vision and pattern recognition*, pages 606–615, 2018. 1
- [7] Xintao Wang, Ke Yu, Shixiang Wu, Jinjin Gu, Yihao Liu, Chao Dong, Yu Qiao, and Chen Change Loy. ESRGAN: Enhanced super-resolution generative adversarial networks. In *Proceedings of the European Conference on Computer Vision (ECCV)*, pages 0–0, 2018. 1, 8
- [8] Wenlong Zhang, Yihao Liu, Chao Dong, and Yu Qiao. RankSRGAN: Generative adversarial networks with ranker for image super-resolution. In *2019 IEEE/CVF International Conference on Computer Vision (ICCV)*, pages 3096–3105, 2019. 1

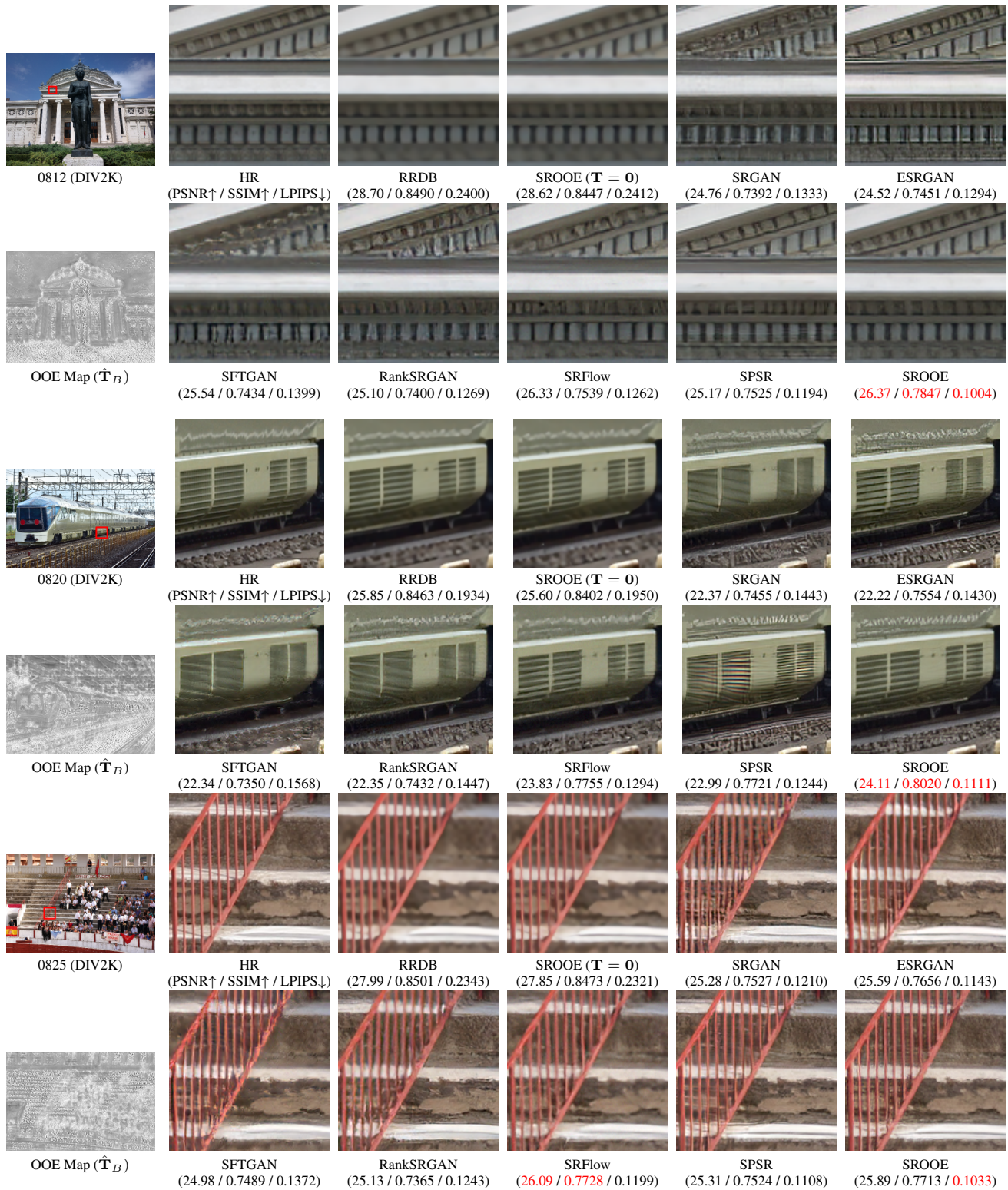


Figure 1. Visual comparison with state-of-the-art methods for $4\times$ SR results. Among the seven perception-oriented SR methods, the best performances are highlighted in red.

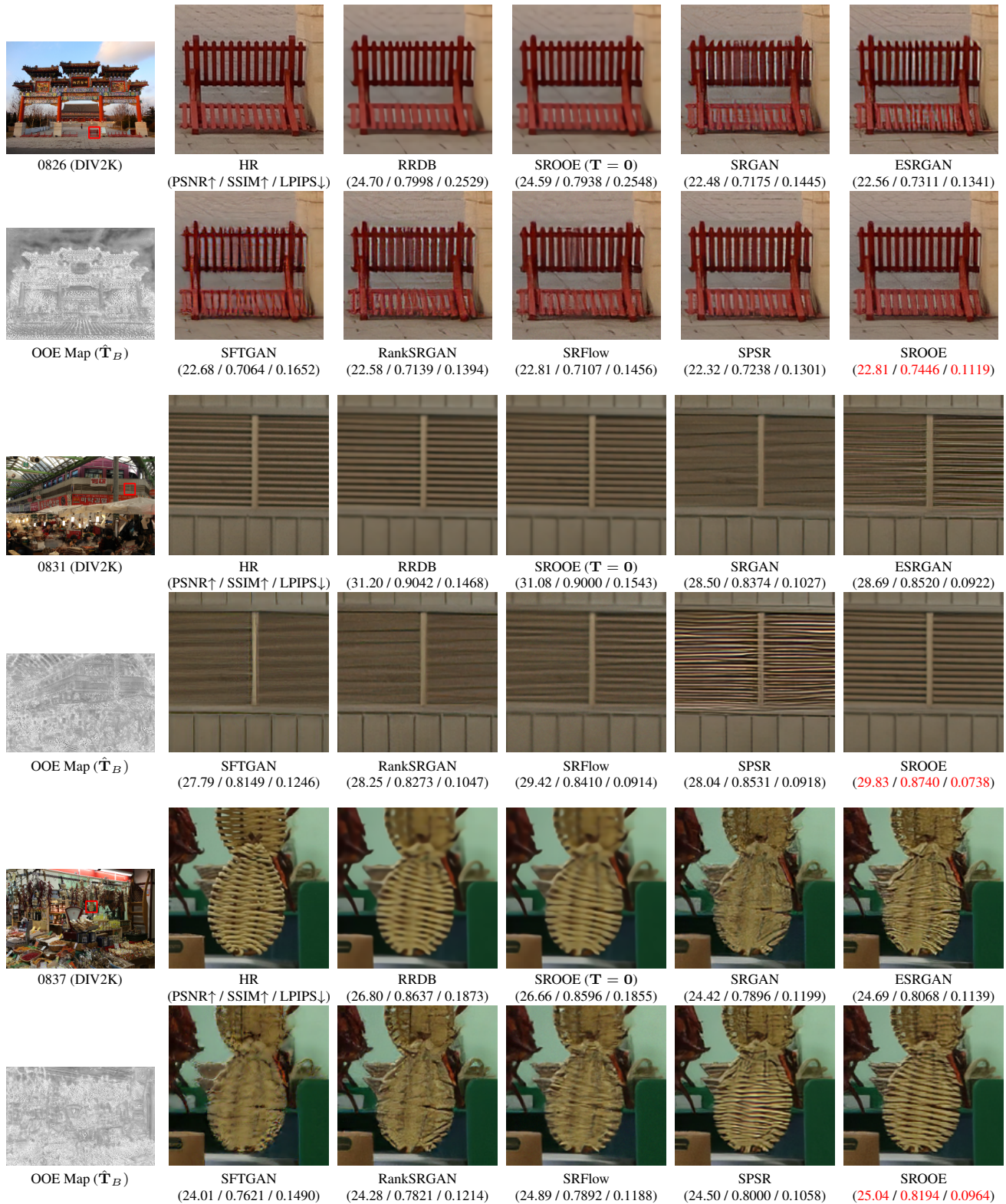


Figure 2. Visual comparison with state-of-the-art methods for $4\times$ SR results. Among the seven perception-oriented SR methods, the best performances are highlighted in red.

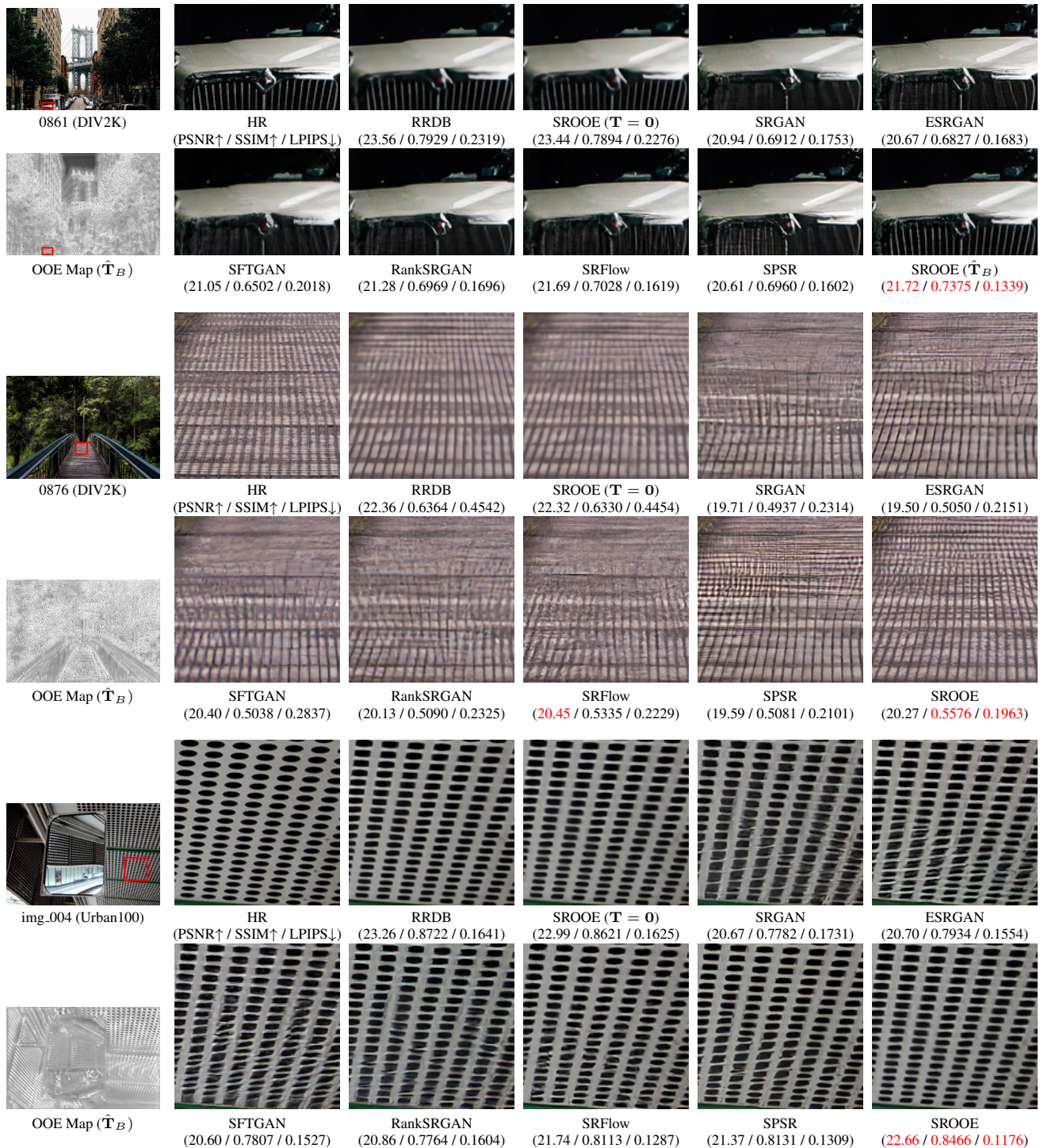


Figure 3. Visual comparison with state-of-the-art methods for $4\times$ SR results. Among the seven perception-oriented SR methods, the best performances are highlighted in red.

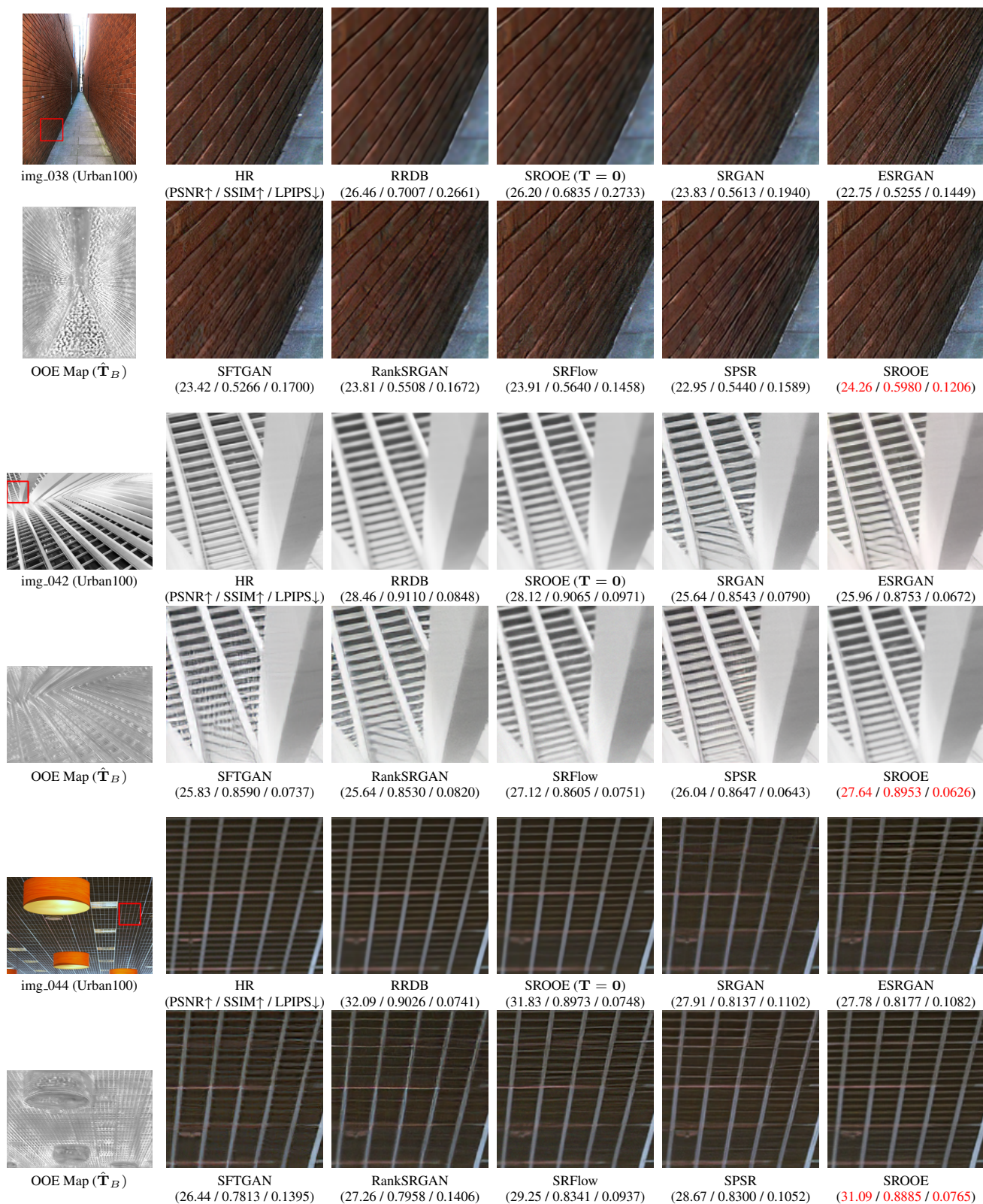


Figure 4. Visual comparison with state-of-the-art methods for 4× SR results. Among the seven perception-oriented SR methods, the best performances are highlighted in red.

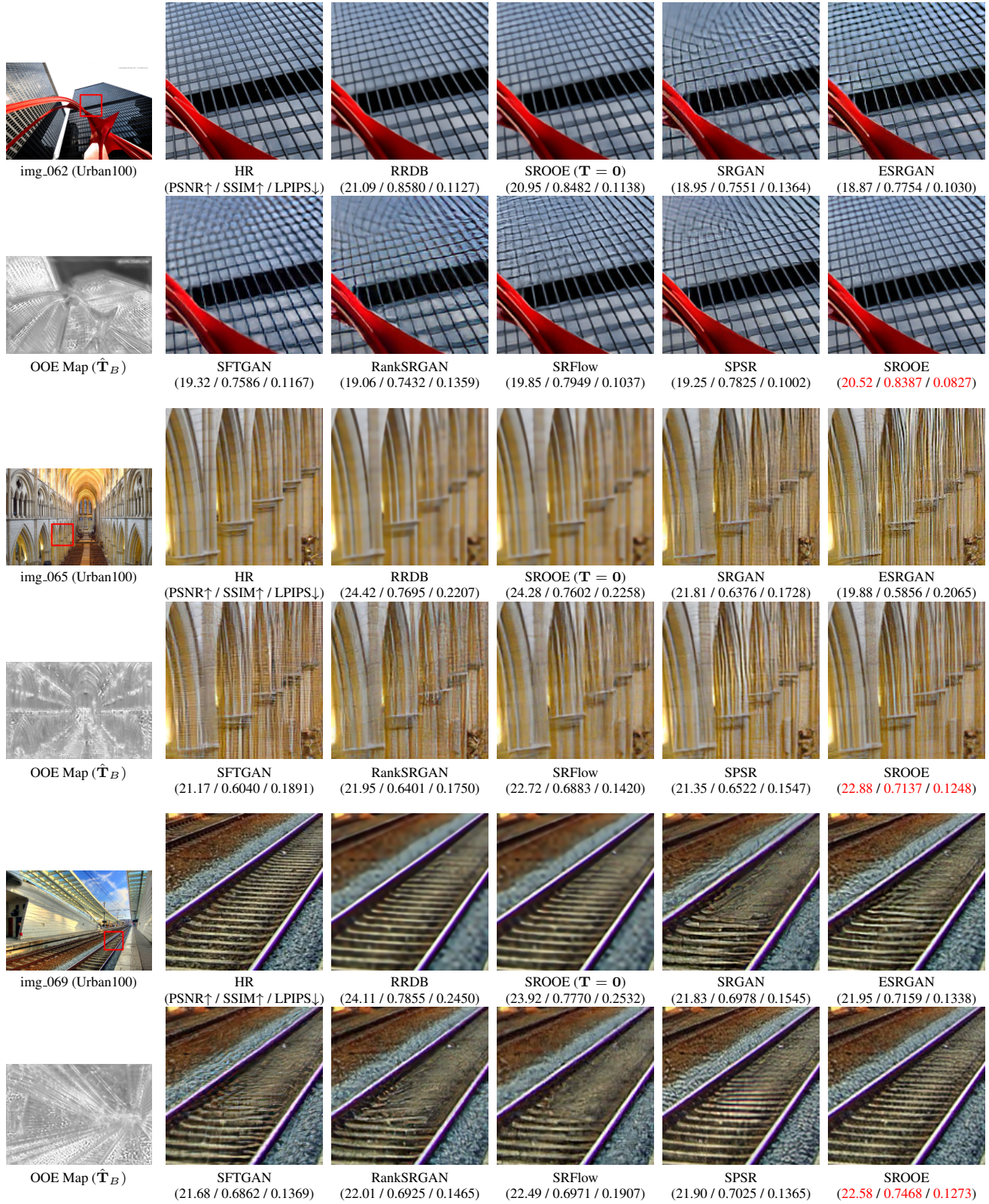


Figure 5. Visual comparison with state-of-the-art methods for $4\times$ SR results. Among the seven perception-oriented SR methods, the best performances are highlighted in red.

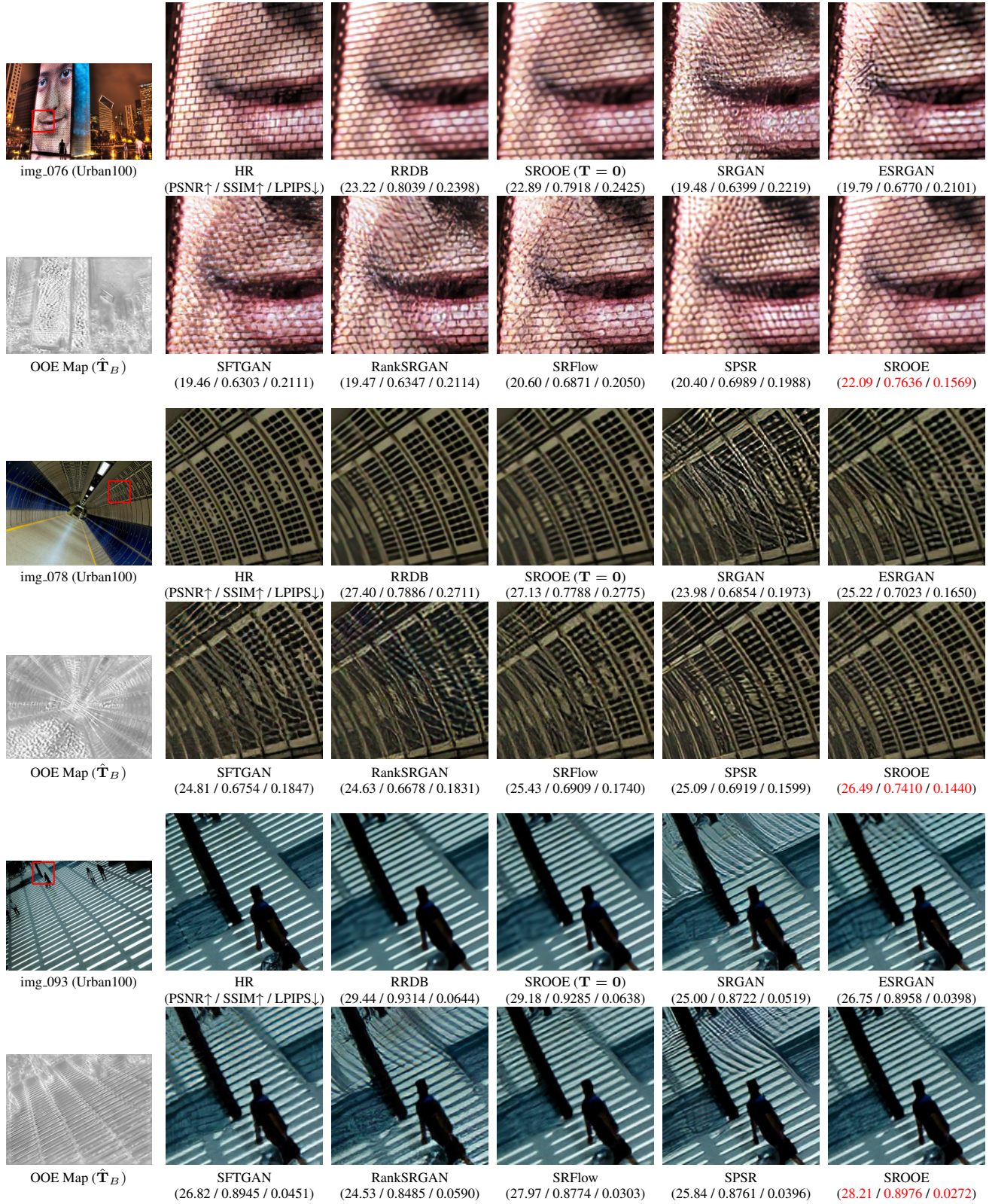


Figure 6. Visual comparison with state-of-the-art methods for 4 \times SR results. Among the seven perception-oriented SR methods, the best performances are highlighted in red.

Table 1. Comparison with state-of-the-art SR $8\times$ methods on benchmarks. The 1st and the 2nd best performances for each group are highlighted in red and blue, respectively. LR-PSNR values greater than 45dB are underlined.

Model		Distortion-oriented SR				Perception-oriented SR			
		RRDB [7]	SRFlow ($\tau = 0$) [3]	FxSR ($\mathbf{T} = \mathbf{0}$) [5]	SROOE ($\mathbf{T} = \mathbf{0}$)	ESRGAN [7]	SRFlow ($\tau = 0.9$) [3]	FxSR ($\mathbf{T} = 0.8$) [5]	SROOE ($\hat{\mathbf{T}}_B$)
Training dataset		DIV2K	DF2K	DIV2K	DF2K	DF2K+OST	DIV2K	DIV2K	DF2K
BSD100	PSNR \uparrow	23.57	23.37	23.60	23.61	21.11	21.66	21.93	22.23
	SSIM \uparrow	0.5708	0.5428	0.5728	0.5718	0.4658	0.4632	0.5039	0.5164
	LPIPS \downarrow	0.5548	0.5303	0.5079	0.5378	0.3103	0.3238	0.3129	0.2996
	DISTS \downarrow	0.2941	0.3183	0.2753	0.2861	0.1881	0.2068	0.1972	0.1891
	LR-PSNR \uparrow	46.23	<u>52.39</u>	<u>47.12</u>	<u>45.34</u>	33.81	<u>51.09</u>	42.41	<u>43.57</u>
Urban100	PSNR \uparrow	21.10	20.91	21.37	21.37	18.82	19.41	19.88	20.17
	SSIM \uparrow	0.5999	0.5735	0.6122	0.6114	0.5005	0.5013	0.5510	0.5696
	LPIPS \downarrow	0.4082	0.3735	0.3454	0.3720	0.2701	0.2965	0.2461	0.2449
	DISTS \downarrow	0.2599	0.2468	0.2193	0.2344	0.1673	0.2039	0.1695	0.1558
	LR-PSNR \uparrow	42.98	<u>50.90</u>	<u>44.28</u>	42.91	29.93	<u>48.94</u>	40.62	<u>42.45</u>
Manga109	PSNR \uparrow	23.05	22.63	23.23	23.26	20.78	20.65	21.86	22.10
	SSIM \uparrow	0.7516	0.7183	0.7527	0.7545	0.6585	0.6439	0.7001	0.7094
	LPIPS \downarrow	0.2457	0.2419	0.2097	0.2242	0.1823	0.2188	0.1640	0.1578
	DISTS \downarrow	0.1495	0.1627	0.1272	0.1339	0.0999	0.1337	0.0980	0.0862
	LR-PSNR \uparrow	43.03	<u>49.16</u>	42.78	42.40	32.09	<u>45.56</u>	40.89	<u>42.45</u>
DIV2K	PSNR \uparrow	25.50	25.09	25.60	25.61	22.58	23.04	23.56	23.92
	SSIM \uparrow	0.6960	0.6589	0.6989	0.6978	0.5891	0.5728	0.6241	0.6377
	LPIPS \downarrow	0.4227	0.4033	0.3857	0.4071	0.2421	0.2719	0.2402	0.2238
	DISTS \downarrow	0.2185	0.2342	0.1953	0.2073	0.1045	0.1386	0.1190	0.1075
	LR-PSNR \uparrow	46.35	<u>51.28</u>	<u>46.96</u>	<u>45.68</u>	33.15	<u>50.26</u>	42.66	<u>44.08</u>

Table 2. Performance comparison of SR results of ESRGAN models with different weight vectors for perceptual loss. Among the objectives in Sets A and B , except for λ_0 , the 1st and the 2nd best performances for each column are highlighted in red and blue.

Set	objec- tive	λ_{per}					L_{per1}					Metric	
		λ_{V12}	λ_{V22}	λ_{V34}	λ_{V44}	λ_{V54}	L_{V12}	L_{V22}	L_{V34}	L_{V44}	L_{V54}	PSNR	LPIPS
	λ_0	[0.0, 0.0, 0.0, 0.0, 0.0]	0.6459	1.8793	3.9235	2.2091	1.2767	25.48	0.1960				
A	λ_1	[1.0, 0.0, 0.0, 0.0, 0.0]	0.8320	2.0275	3.8340	1.9804	1.0480	23.95	0.1124				
	λ_2	[0.0, 1.0, 0.0, 0.0, 0.0]	0.8322	1.9523	3.6789	1.9200	1.0171	23.84	0.1125				
	λ_3	[0.0, 0.0, 1.0, 0.0, 0.0]	0.8565	2.0222	3.5480	1.8452	0.9841	23.66	0.1124				
	λ_4	[0.0, 0.0, 0.0, 1.0, 0.0]	0.8844	2.0977	3.7413	1.8777	0.9890	23.28	0.1158				
	λ_5	[0.0, 0.0, 0.0, 0.0, 1.0]	0.9051	2.1593	3.8985	1.9565	1.0085	23.00	0.1232				
B	λ_1	[1.0, 0.0, 0.0, 0.0, 0.0]	0.8320	2.0275	3.8340	1.9804	1.0480	23.95	0.1124				
	λ_{1-2}	[1/2, 1/2, 0.0, 0.0, 0.0]	0.8112	1.9432	3.6740	1.9114	1.0125	24.08	0.1075				
	λ_{1-3}	[1/3, 1/3, 1/3, 0.0, 0.0]	0.8468	1.9964	3.5846	1.8532	0.9821	23.81	0.1112				
	λ_{1-4}	[1/4, 1/4, 1/4, 1/4, 0.0]	0.8474	2.0085	3.6174	1.8489	0.9765	23.68	0.1110				
	λ_{1-5}	[1/5, 1/5, 1/5, 1/5, 1/5]	0.8439	2.0085	3.6174	1.8515	0.9821	23.74	0.1114				

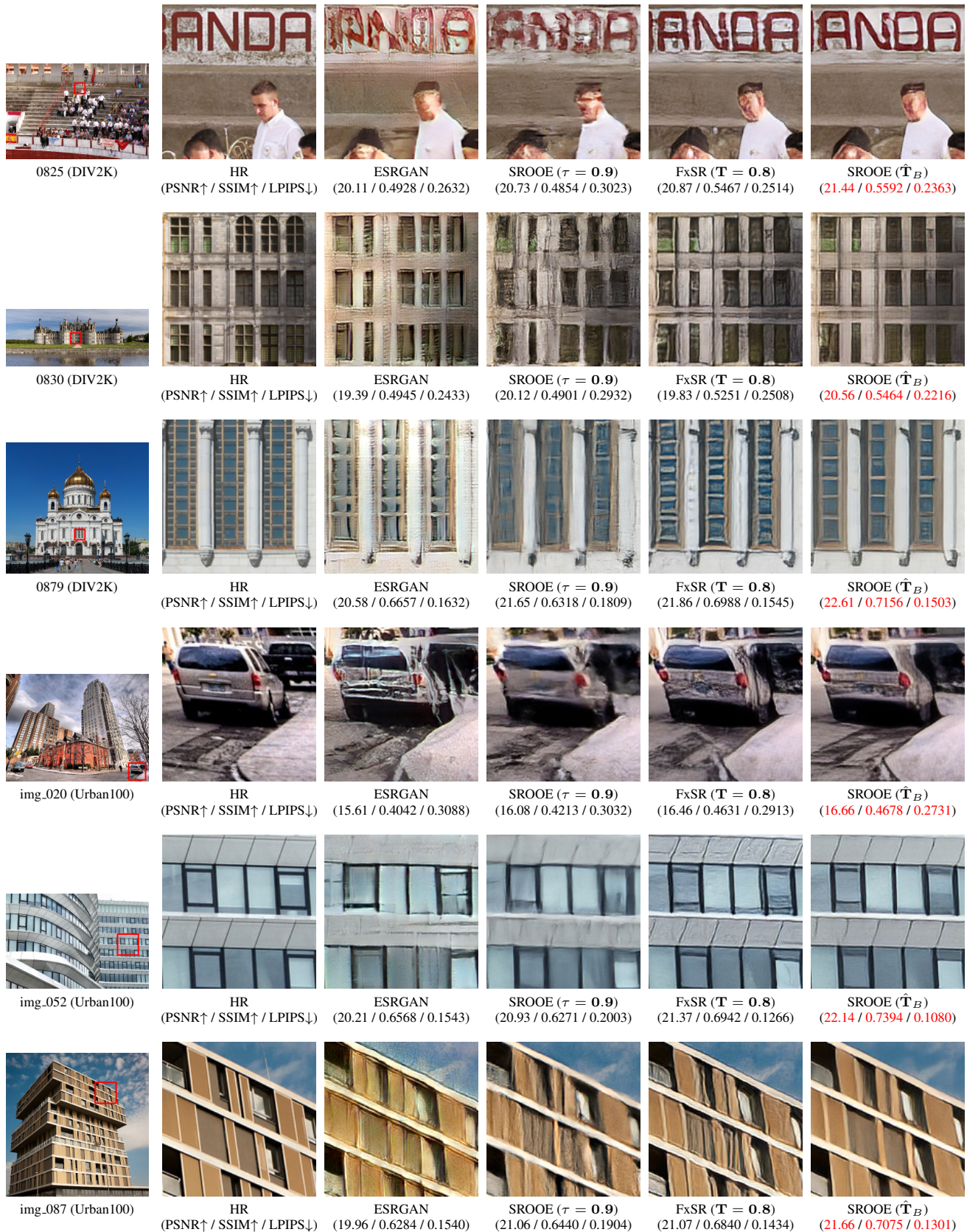


Figure 7. Visual comparison with state-of-the-art methods for $8\times$ SR results. Among the four perception-oriented SR methods, the best performances are highlighted in red.



Figure 8. Visual comparison with state-of-the-art methods for $8\times$ SR results. Among the four perception-oriented SR methods, the best performances are highlighted in red.